Mutation Research 644 (2008) 48–55

Contents lists available at ScienceDirect

Mutation Research/Fundamental and Molecular Mechanisms of Mutagenesis

journal homepage: www.elsevier.com/locate/molmut
Community address: www.elsevier.com/locate/mutres

The tumor suppressor homolog in fission yeast, *myh1*$^+$, displays a strong interaction with the checkpoint gene *rad1*$^+$

Kristina Jansson[a], Jonas Warringer[a], Anne Farewell[a], Han-Oh Park[b], Kwang-Lae Hoe[c], Dong-Uk Kim[c], Jacqueline Hayles[d], Per Sunnerhagen[a,*]

[a] *Department of Cell and Molecular Biology, Lundberg Laboratory, Göteborg University, P.O. Box 462, Göteborg SE-405 30, Sweden*
[b] *Bioneer Corporation, 49-3, Munpyeong-dong, Daedeok-gu, Daejon 306-220, Republic of Korea*
[c] *Functional Genomics Research Center, Korea Research Institute of Bioscience and Biotechnology (KRIBB), Yusong, Daejeon, Republic of Korea*
[d] *Cell Cycle Laboratory, Cancer Research UK, London Research Institute, 44 Lincoln's Inn Fields, London WC2A 3PX, United Kingdom*

ARTICLE INFO

Article history:
Received 4 March 2008
Received in revised form 2 June 2008
Accepted 3 July 2008
Available online 16 July 2008

Keywords:
DNA repair
DNA glycosylase
Base-excision repair
UV sensitivity
9-1-1 complex

ABSTRACT

The DNA glycosylase MutY is strongly conserved in evolution, and homologs are found in most eukaryotes and prokaryotes examined. This protein is implicated in repair of oxidative DNA damage, in particular adenine mispaired opposite 7,8-dihydro-8-oxoguanine. Previous investigations in *Escherichia coli*, fission yeast, and mammalian cells show an association of mutations in MutY homologs with a mutator phenotype and carcinogenesis. Eukaryotic MutY homologs physically associate with several proteins with a role in replication, DNA repair, and checkpoint signaling, specifically the trimeric 9-1-1 complex.

In a genetic investigation of the fission yeast MutY homolog, *myh1*$^+$, we show that the *myh1* mutation confers a moderately increased UV sensitivity alone and in combination with mutations in several DNA repair genes. The *myh1 rad1*, and to a lesser degree *myh1 rad9*, double mutants display a synthetic interaction resulting in enhanced sensitivity to DNA damaging agents and hydroxyurea. UV irradiation of *myh1 rad1* double mutants results in severe chromosome segregation defects and visible DNA fragmentation, and a failure to activate the checkpoint. Additionally, *myh1 rad1* double mutants exhibit morphological defects in the absence of DNA damaging agents. We also found a moderate suppression of the slow growth and UV sensitivity of *rhp51* mutants by the *myh1* mutation.

Our results implicate fission yeast Myh1 in repair of a wider range of DNA damage than previously thought, and functionally link it to the checkpoint pathway.

1. Introduction

In order to minimize the rate of genome alteration, several DNA repair pathways combine to recognize and remove damaged sites. The efficacy of this process is not only dependent on the individual repair proteins, but also on coordination of DNA repair with other cellular processes including regulation of transcription of genes required for DNA repair and stress survival, and of cell cycle progression. The requirement to eliminate damage before it could potentially be fixed into a mutation by DNA replication can be met by increasing DNA repair efficiency, and by decreasing proliferation rates, allowing more time to pass between successive replications. Both these coordination tasks are performed in eukaryotes by the DNA-dependent checkpoint pathway.

The bulk of DNA repair is carried out by the nucleotide excision repair (NER) and base-excision repair (BER) pathways, both of which operate on damage induced by external agents such as irradiation, alkylating or oxidizing chemicals, or by replication errors. The BER pathway relies on recognition of DNA damage by DNA glycosylases, which excise the damaged base by breaking the glycosidic bond between base and the deoxyribose moiety. In subsequent steps, the remaining sugar–phosphate residue is removed, and the resulting gap can be either filled directly or first extended and subsequently filled. For a review of BER, see [1]. The *Escherichia coli* MutY protein is a DNA glycosylase which acts to remove adenine misincorporated opposite oxidatively damaged residues, mainly 7,8-dihydro-8-oxoguanine (8-oxoG), from DNA. Another glycosylase, MutM, is capable of removing 8-oxoG itself from 8-oxoG:C base pairs [2]. The *E. coli mutY* mutation was originally isolated on basis of its mutator phenotype [3].

MutY homologs are highly conserved among both prokaryotes and eukaryotes and are present in most sequenced genomes, with

* Corresponding author. Tel.: +46 31 786 3830; fax: +46 31 786 3801.
E-mail address: per.sunnerhagen@cmb.gu.se (P. Sunnerhagen).

0027-5107/$ – see front matter © 2008 Elsevier B.V. All rights reserved.
doi:10.1016/j.mrfmmm.2008.07.001

the notable exception of *Saccharomyces cerevisiae*. The *Schizosaccharomyces pombe myh1*$^+$ gene encodes a 53-kDa protein with high sequence similarity to both *E. coli* MutY and the human homolog [4]. Like *E. coli* MutY, *S. pombe* Myh1 has activity *in vitro* towards adenine mismatched with 8-oxoG [4,5] In keeping with the role of MutY homologs in repair of oxidative damage, *S. pombe myh1* mutants are moderately sensitive to hydrogen peroxide and have a pronounced mutator phenotype like *E. coli mutY* mutants [6]. The human and *S. pombe* MutY homologs have been reported to physically interact with all three members of the checkpoint "9-1-1" sensor complex, Rad9, Rad1, and Hus1 individually [7,8]. Physical interactions also exist between Myh1 and PCNA, the trimeric DNA polymerase clamp [9], which has structural similarities to the "9-1-1" proteins [10]. Further, MutY homologs in *E. coli* and human cells have been reported to bind the mismatch repair protein MutS and its human homolog Msh6, respectively [11,12].

Inherited mutations in the human MutY homologous gene, *MYH*, have been found associated with familial adenomatous polyposis (FAP) [13–15]. The majority, ~80%, of FAP cases carry mutations in the *APC* gene; *MYH* mutations are found in a large fraction of the remaining FAP cases [13,16]. Germline mutations in *MYH* may account for up to 1–3% of all colorectal cancer [16,17]. The link between *MYH* deficiencies and carcinogenesis is further strengthened by studies in mice, where *MYH* mutations in combination with mutations in *OGG1* result in predisposition to cancer, predominantly in the lung [18]. More recent work reports increased disposition to intestinal malignancies in *myh* single mutant mice [19].

Despite these demonstrations of physical interactions between eukaryotic MutY homologs and members of the 9-1-1 complex on one hand, and the genetic evidence linking human *MYH* mutations to familial adenomatous polyposis, little is understood of the functional DNA repair pathways in which eukaryotic MutY homologs participate, nor to which DNA damaging agents MutY homologs are required for survival. In the present study, we set out to map the role of the eukaryotic MutY homolog in DNA repair and checkpoint pathways, using genetic experiments in fission yeast where the *myh1* mutation is studied in combination with mutations in other DNA repair and checkpoint genes. We find that the *S. pombe myh1*$^+$ gene contributes to survival after UV irradiation in a number of genetic backgrounds, adding to its previously demonstrated role in repair of oxidative damage. In *myh1* mutants, the checkpoint response becomes activated by far lower UV doses than in wild-type (wt) cells. Deletion of *myh1*$^+$ and the checkpoint gene *rad1*$^+$ yields an extremely UV- and methyl methane sulfonate (MMS) sensitive double mutant. In addition to its UV sensitivity, the *myh1 rad1* double mutant displays very low viability in the presence of the replication inhibitor hydroxyurea (HU), and morphological aberrations.

2. Materials and methods

2.1. Fission yeast genetic techniques

All experiments were carried out in the haploid *h*$^-$ *leul-32 ura4-D18 ade6-M210/M216* background provided by the Korean Research Institute for Bioscience and Biotechnology (KRIBB) and Bioneer Corporation. Gene deletion cassettes carrying the *hphMX6* hygromycin resistance marker [20] were constructed with PCR using hybrid primers with 80 nucleotide homology to the chromosomal locus Table 2. Chromosomal gene deletions were introduced by homologous recombination and transformation as described [21]. All gene deletions were verified by PCR using primers in flanking chromosomal DNA.

2.2. Exposure to DNA damage and DNA synthesis inhibition

For UV sensitivity measurements, cells were grown to stationary phase in synthetic complete (SC) medium [22] supplemented with histidine, tryptophan and uracil at 40 mg/l each, adenine at 60 mg/l and leucine at 150 mg/l. Alternatively, cells were grown to mid-exponential phase (A_{595nm} = 0.5). The different strains were adjusted to the same cell density, serially diluted, and 4 μl droplets were deposited on SC agar plates. Irradiation with 254 nm UV light was done with a UVGL-58 short wave UV lamp (UV Products, San Gabriel, Calif.). The dose rate was 2 W/m^2, which was monitored with a UVX digital UV meter (UV Products). HU sensitivity was measured on SC agar plates containing 5 mM of HU.

2.3. Micro-cultivation and analysis of synergism

Single and double deletion strains were pre-cultivated in micro-scale (350 μl) for two serial rounds (2× 48 h) in liquid YES (0.5 % (w/v) yeast extract, 3 % (w/v) glucose, 225 mg/l each of histidine, lysine, uracil, adenine and leucine) medium. For experimental cultures, strains were inoculated to an optical density (OD) of 0.07–0.15 in 350 μl of YES medium (as above, except when glucose was replaced with alternative carbon sources as indicated below), with or without chemicals and micro-cultivated for 72 h in 30 °C in a Bioscreen Analyzer C (Growth Curve Oy, Finland) as earlier described for *S. cerevisiae* strains [23]. Strain replicates in drugs n = 2 (n = 4 for wt), strain replicates in no stress = 10 (n = 20 for wt). Drug concentrations were set as to equal a 50–100% increase in population doubling time in the wt. This corresponded to the following concentrations: $CoCl_2$, 0.25 mM; $BaCl_2$, 8.5 mM, $CdCl_2$, 0.25 μM; $CuCl_2$, 0.75 mM; diamide 0.15 mg/ml; NaCl, 0.1 M; paraquat, 0.2 mg/ml; $MnCl_2$, 0.1 mM; $AlCl_3$, 0.2 mg/ml; $Pb(NO_3)_2$, 0.4 mM; cycloheximide, 5 μg/ml; mal-

Table 1
S. pombe strains used in this study

Strain	Genotype	Source
ED666	*h*$^-$ *leul-32 ura4-D18 ade6-M210/M216*	KRIBB/Bioneer
BG1190 216	*h*$^-$ *myh1Δ::kanMX leul-32 ura4-D18 ade6-M210/M216*	KRIBB/Bioneer
BG0649 216	*h*$^-$ *rad1Δ::kanMX leul-32 ura4-D18 ade6-M210/M216*	KRIBB/Bioneer
RAD1MYH1 110	*h*$^-$ *rad1Δ::kanMX myh1Δ::hphMX6 leul-32 ura4-D18 ade6-M210/M216*	This work
BG0827 216	*h*$^-$ *hus1Δ::kanMX leul-32 ura4-D18 ade6-M210/M216*	KRIBB/Bioneer
HUS1MYH1 102	*h*$^-$ *hus1Δ::kanMX myh1Δ::hphMX6 leul-32 ura4-D18 ade6-M210/M216*	This work
BG1918 216	*h*$^-$ *rad9Δ::kanMX leul-32 ura4-D18 ade6-M210/M216*	KRIBB/Bioneer
RAD9MYH1 103	*h*$^-$ *rad9Δ::kanMX myh1Δ::hphMX6 leul-32 ura4-D18 ade6-M210/M216*	This work
BG0317 216	*h*$^-$ *rad17Δ::kanMX leul-32 ura4-D18 ade6-M210/M216*	KRIBB/Bioneer
RAD17MYH1 105	*h*$^-$ *rad17Δ::kanMX myh1Δ::hphMX6 leul-32 ura4-D18 ade6-M210/M216*	This work
CHK1 101	*h*$^-$ *chk1Δ:: hphMX6 leul-32 ura4-D18 ade6-M210/M216*	This work
MYH1CHK1 115	*h*$^-$ *myh1Δ::kanMX chk1Δ::hphMX6 leul-32 ura4-D18 ade6-M210/M216*	This work
BG1575 216	*h*$^-$ *rad2Δ::kanMX leul-32 ura4-D18 ade6-M210/M216*	KRIBB/Bioneer
RAD2MYH1 101	*h*$^-$ *rad2Δ::kanMX myh1Δ::hphMX6 leul-32 ura4-D18 ade6-M210/M216*	This work
BG3621 216	*h*$^-$ *rad13Δ::kanMX leul-32 ura4-D18 ade6-M210/M216*	KRIBB/Bioneer
RAD13MYH1 104	*h*$^-$ *rad13Δ::kanMX myh1Δ::hphMX6 leul-32 ura4-D18 ade6-M210/M216*	This work
BG1906 216	*h*$^-$ *rhp51Δ::kanMX leul-32 ura4-D18 ade6-M210/M216*	KRIBB/Bioneer
RHP51MYH1 109	*h*$^-$ *rhp51Δ::kanMX myh1Δ::hphMX6 leul-32 ura4-D18 ade6-M210/M216*	This work
RHP18 107	*h*$^-$ *rhp18Δ:: hphMX6 leul-32 ura4-D18 ade6-M210/M216*	This work
MYH1RHP18 102	*h*$^-$ *myh1Δ::kanMX rhp18Δ::hphMX6 leul-32 ura4-D18 ade6-M210/M216*	This work
BG4656 210	*h*$^-$ *msh6Δ::kanMX leul-32 ura4-D18 ade6-M210/M216*	KRIBB/Bioneer
MSH6MYH1 102	*h*$^-$ *msh6Δ::kanMX myh1Δ::hphMX6 leul-32 ura4-D18 ade6-M210/M216*	This work

tose, 3% (glucose substituted); galactose, 3% (glucose substituted); doxorubicin, 15 μg/ml; *tert*-butyl hydroperoxide, 0.07%; raffinose, 3% (glucose substituted); 6-azauracil, 0.2 mg/ml; CsCl, 4 mg/ml; $NiCl_2$, 0.2 mM; $HqCl_2$, 0.01 mM; anisomycin, 7.5 μg/ml; trifluperazine, 50 μM; tellurite, 0.5 mM; arsenite, 25 mM; selenite, 1 mM; ethanol (tolerance), 7%; ethanol (growth), 3% (glucose substituted); glycerol, 3% (glucose substituted); MMS, 0.015%; HU, 0.8 mg/ml; KCl, 0.9 M.

OD measurements were taken every 20 min during a 72–80-h period resulting in growth curves. Growth curves were calibrated, and for each curve the variable growth rate was extracted as described earlier [23]. For each condition, the growth rate (doubling time) of each strain, single or double mutant, was compared and normalized to that of the corresponding wt replicates, forming normalized growth rate ratios referred to as Logarithmic Strain Coefficient (LSC) [23] and roughly corresponding to ln (doubling time wt/doubling time knockout). To distinguish growth aberrations in the presence of drugs from general growth aberrations present already in no stress conditions, a Logarithmic Phenotypic Index (LPI), was formed for each knockout in each drug, likewise described earlier [23]. The LPI corresponds to $LSC_{drug} - LSC_{no\ stress}$. To investigate whether a given double deletion strain is more or less sensitive to a given stress than what is expected from the behavior of the individual single deletion strains, a multiplicative model (additive on log-scale) was applied. $LPI_{xy} = LPI_x + LPI_y$ was thus considered to reflect no interactions between genes, $LPI_{xy} < LPI_x + LPI_y$ reflected a synergistic interaction, and $LPI_{xy} > LPI_x + LPI_y$ an antagonistic interaction, where LPI_{xy} is the growth aberration of the double deletion relative the wt and LPI_x and LPI_y the growth aberration of the respective single deletions relative to the wt.

2.4. Microscopy

All microscopy was done on a Zeiss Axioplan 2. General cell morphology was visualized on native cells in bright-field and Nomarski optics at 100× magnification. For measurement of septation indices, cells were fixed in 70% ethanol and scored in bright-field. Chromosomes were visualized at 100× magnification by staining with 4′,6-diamidino-2-phenylindol dihydrochloride (DAPI) as described [24].

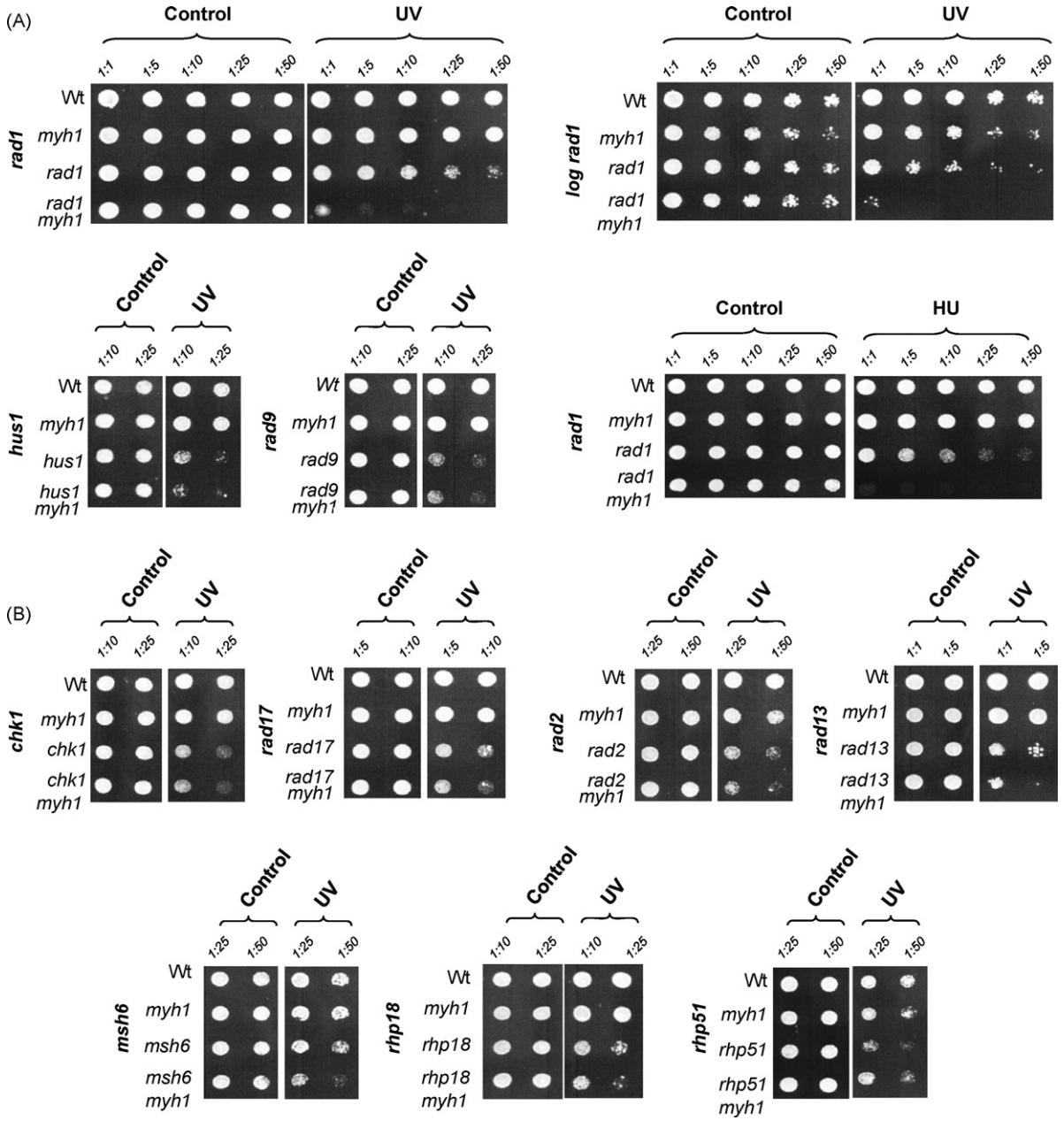

Fig. 1. UV and HU sensitivity of *myh1* single and double mutants as measured on plate spot assays reveal an interaction between *myh1* and *rad1*. Cells were grown to stationary phase (except where indicated in top right panel), diluted on SC plates as indicated and UV irradiated or grown on SC plates containing 5 mM HU (as indicated). For each pair of panels, untreated cells are shown to the left and irradiated or HU-treated to the right. The following doses of UV were used for the different mutant sets: *rad1*, 120 J/m^2; *rad1* log phase, 60 J/m^2 *rad2*, 120 J/m^2; *rad13*, 120 J/m^2; *rad17*, 60 J/m^2; *rad9*, 60 J/m^2; *chk1*, 120 J/m^2; *msh6*, 120 J/m^2; *rhp18*, 240 J/m^2; *rhp51*, 240 J/m^2. (A) 9-1-1 sensor complex mutants. "Log rad1", *rad1* mutants in logarithmic phase growth. (B) Other checkpoint mutants and DNA repair mutants.

3. Results

3.1. Genetic interactions between myh1 and DNA repair mutations

In order to obtain an overview of the repair processes where *myh1*$^+$ might be involved, we created double null mutants with homologous recombination combining *myh1* with representatives of different DNA repair pathways. Thus, *myh1*$^+$ was deleted in the *rad1* (checkpoint-defective) background, as well as in the *rad2* (defective in long-patch BER and the alternative UV damage excision repair pathway), *rad13* (NER), *rhp51* (homologous recombination), *msh6* (mismatch repair), and *rhp18* (postreplication repair) backgrounds (Table 1). For each single and double mutant strain, UV sensitivity was investigated by spot assays. In line with earlier results [6], the *myh1* single mutant was not visibly UV sensitive (Fig. 1). For most of these mutant combinations, the double mutant was equally sensitive or only slightly more sensitive than the more sensitive of the single mutants. Two exceptions were obvious. First, *rhp51 myh1* double mutants were somewhat less UV sensitive than *rhp51* single mutants, indicating suppression of the *rhp51* mutation by *myh1*. In line with this, the slow growth phenotype of *rhp51* single mutants was rescued by the *myh1* mutation (not shown). Second, *rad1 myh1* double mutants were significantly more UV sensitive than *rad1* single mutants, indicating a strong synthetic interaction between *myh1* and this checkpoint mutation.

We wanted to further investigate the *rad1 myh1* interaction, and so created double mutants combining *myh1* with other checkpoint pathway mutations: *hus1*, *rad9*, *rad17*, and *chk1*. None of the other combinations displayed a strong synthetic interaction; the double mutants were either equally sensitive or slightly more sensitive than the corresponding single checkpoint mutant (see Fig. 1). We did note a slight growth rate defect for all *myh1-checkpoint* double mutants, however, including *rad1 myh1*.

Checkpoint mutants are generally more sensitive to DNA damaging agents when actively passing through the cell cycle than in a non-dividing state. We tested the UV sensitivity of *rad1 myh1* mutants and the cognate single mutants in mid-exponential growth phase. As expected, *rad1* mutants appeared considerably more sensitive (Fig. 1). A slight sensitivity was also visible for the *myh1* single mutant under these conditions. Most strikingly, however, *rad1 myh1* double mutants were extremely sensitive. We also wished to examine if the *myh1* mutation would affect sensitivity to replication inhibitors such as HU, since many *S. pombe* checkpoint mutants are also HU sensitive. As seen in Fig. 1, while *rad1* mutants were sensitive to growth on HU-containing medium as expected, *rad1 myh1* double mutants were exceedingly HU sensitive. The *myh1* single mutants displayed wt resistance.

3.2. Sensitivity profiling of double mutants with myh1 reveal additional sensitivities and interaction with rad9

We wanted to see if our findings with UV radiation and HU could be extended to other DNA-damaging agents, which would give additional information about the types of DNA damage where Myh1 plays a role in repair. Thus, we exposed the wt, all single mutants, and all *myh1* double mutants to a range of genotoxic compounds in liquid culture, and recorded the growth defects. As expected, several checkpoint single mutants were highly sensitive to HU and MMS (Fig. 2A). Among the *myh1–x* double mutants, a clear synthetic phenotype was seen for *myh1 rad1*, in agreement with the results from plate tests. In addition, a synthetic phenotype was seen for *myh1 rad9* (Fig. 2B). As judged by this more sensitive test, both *myh1 rad1* and *myh1 rad9* were more susceptible to both HU and MMS than the *rad1* or *rad9* single mutants, respectively, which is

Table 2
Sequences of oligonucleotides used for generation of genomic disruptions

Name	Homologies	Sequence (5′–3′)
MYH1HphMXPF	−79 to 0 (MYH1) and −420 to −401 (HphMX6)	CCCTTCAACACTAGTTTTCTCTTTCTTTTCCGTTTCATGTTTACTTTCTTTTATTAATTGTATATATATTTAATTTAGCGGATCCCCGGGTTAATTAA
MYH1HphMXPR	1527–1607 (MYH1) and 1262–1282 (HphMX6)	TTGAAGAATGGGATAAAGATTATTTCCCAAAAAGGCTAATAGAAGAATTAAAAGGAGAATTGTCGAAAACAAAGGCGTGAGAATTCGAGCTCGTTTAAAC
CHK1KanMXPF	−81 to 0 (CHK1) and −416 to −396 (KanMX6)	CCTTACCATATTGGTAGAGAAATACGTACTGGGGCTTTTGCTTCCGTCCGTTTATGTTACGATGATAATGCTAAAATATATGCGGATCCCCGGGTTAATTAA
CHK1KanMXPR	1757–1838 (CHK1) and 1043–1063 (KanMX6)	TTAATTTTGTGAAACATCTGTAACAACAATCGGCTTCCCTATTGAACTGACAACGTTTTTAAAAAATTTTCTCCATTCAAGGAATTCGAGCTCGTTTAAAC
RHP18HphMXPF	−79 to 0 (RHP18) and −420 to −401 (HphMX6)	GAGAGTGCTCTTACGAATCCCTAATTAAGTTTGAATATTAGTGCATATTAACTATTAATGGGTTTGCAATTTAAAATAAGCGGATCCCCGGGTTAATTAA
RHP18HphMXPR	1164–1245 (RHP18) and 1262–1282 (HphMX6)	GTGATTATATATAGCCAAATAAACTAATAAGTTAATCTGATAATGAAAATTCGTTAAAACCAATCCAACCAAAATTAATGAGAATTCGAGCTCGTTTAAAC

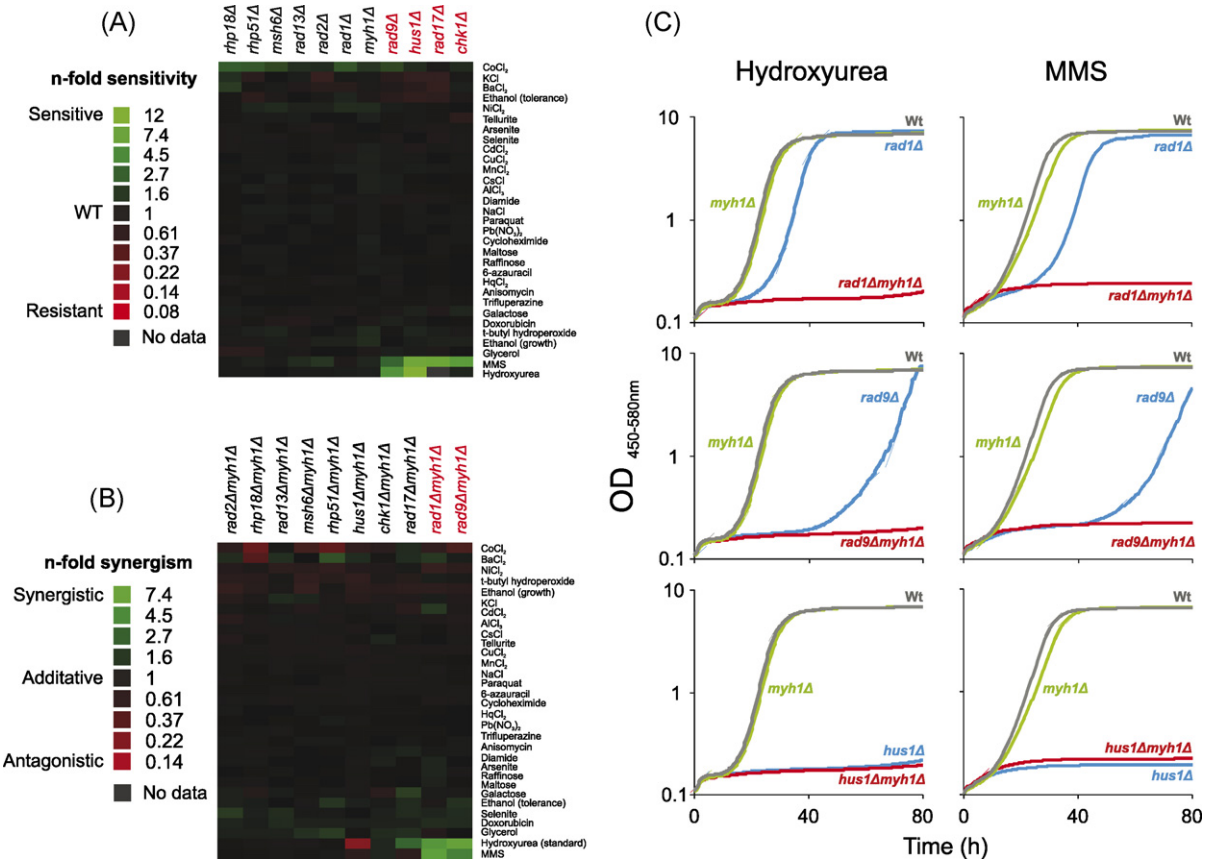

Fig. 2. Quantifying growth rate aberrations and gene–gene synergism of single and *myh1–x* double deletions in liquid culture reveals additional genetic interactions. (A) Growth rate aberrations (LPI) of single deletion strains in an array of environmental conditions. Green = single deletion strain sensitivity, red = single deletion strain resistance. (B) Gene–gene interactions, $LPI_{xy} - LPI_x - LPI_y$ where LPI_{xy} is the growth aberration of the double deletion relative the wt and LPI_x and LPI_y the growth aberration of the respective single deletions relative the wt. Green = synergistic interaction, red = antagonistic interaction. (C) Growth of wt, *rad1*Δ, *rad9*Δ, *myh1*Δ and *hus1*Δ single deletion strains and the corresponding *myh1*Δ double deletion strains exposed to HU or MMS.

also seen in the individual growth curves for the respective mutants (Fig. 2C). Neither *myh1 rad1* nor *myh1 rad9* double mutants were sensitive to any of the non-genotoxic compounds tested, however (Fig. 2B).

3.3. The myh1 rad1 double mutant displays aberrant morphology

Because of the consistent high sensitivity of the *myh1 rad1* double mutant to DNA-damage and replication stress, we wanted to investigate this mutant in more depth. In bright-field and Nomarski optics, we noticed that *myh1 rad1* double mutants had greatly varying cell shapes, in the presence or absence of DNA damage. While just over half the population appeared largely normal, a very large fraction (about 40%) was not. This population was heterogeneous, with club-like swollen, and shortened cells as the most common types (Fig. 3A and data not shown). No such cells were found in wt or *myh1* mutants. The *rad1* mutants appeared shorter and more rounded than wt, as shown earlier [25]; however no *rad1* cells displayed the club-like morphology characteristic of *myh1 rad1* double mutants (Fig. 3A and data not shown). This was unexpected, as neither *myh1* nor *rad1* mutants, nor mutants of their homologous genes in other organisms, have previously been implicated in cell morphogenesis.

3.4. UV elicits a stronger checkpoint response in myh1 mutants

In response to DNA damage, wt *S. pombe* cells will delay cell cycle progression as a result from activation of the checkpoint pathway. Since most *S. pombe* cells in an asynchronous population are in the G2 phase, this will be manifested as a reduced fraction of cells passing through mitosis. The appearance of cells having laid down a septum is used as a convenient marker for passage through mitosis, and so asynchronous wt cells exposed irradiation will display a depression of the number of septated cells lasting for several hours [26]. This expected behavior was seen in the wt strain (Fig. 4). The *myh1* mutants, exposed to the same UV dose, displayed a more vigorous DNA damage response in that the reduction of septated cells started earlier and reached lower septation indices than in the wt (Fig. 4). Another aspect of the wt checkpoint response is cell elongation, as cell growth continues in the absence of division [26]. We noted that *myh1* cells exposed to the same UV dose (240 J/m^2) elongate about 15% more than the wt; the average length of *myh1* mutants was 17 μm vs. 15 μm for the wt (data not shown).

3.5. The myh1 rad1 double mutant has a severely defective DNA damage response

Fission yeast mutants lacking an intact checkpoint pathway do not elongate upon DNA damage and fail to delay cell cycle progression [26,27]. Instead, they undergo a transient increase in the number of cells passing mitosis ("mitotic burst") [26,28]. This behavior was observed with *rad1* single mutants, as expected (Fig. 4). The *myh1 rad1* double mutants, exposed to the same UV dose as the other strains, displayed a very high proportion of cells with failed mitoses, bisected nuclei, and fragmented chromosomes (not shown). The number of mitotic cells did not decrease with

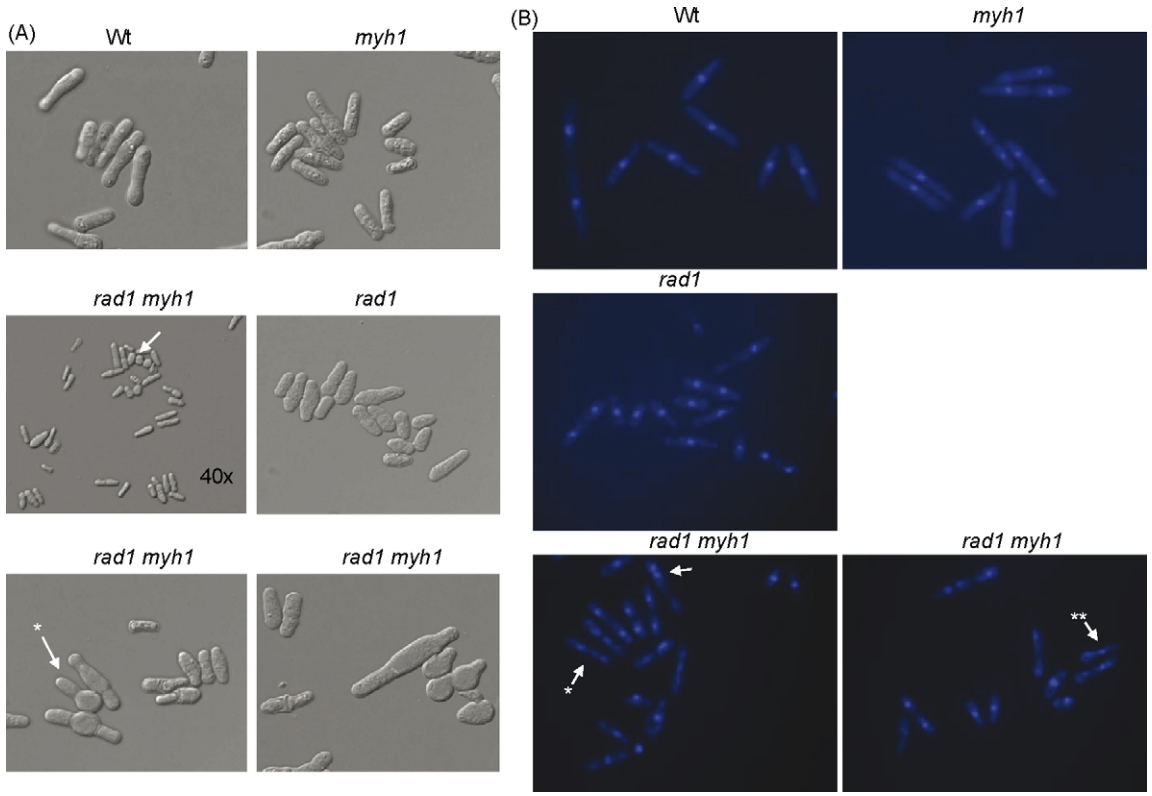

Fig. 3. Morphological defects and chromosomal aberrations after DNA damage in *rad1 myh1* double mutants. Micrographs of *rad1*, *myh1*, and *rad1 myh1* mutant cells, as indicated. Magnification is 100×, or 40× where indicated. (A) Bright-field images of untreated cells →, severely shortened *rad1 myh1* double mutant cell; *→, club-like morphology. (B) Images of DAPI-stained UV-irradiated cells. →, missegregated chromosomes in *rad1 myh1* double mutants; *→, fragmented chromosomal material; **→, bisected nucleus.

time in these mutants (not shown), and so they may be the result of catastrophic attempts at mitosis from which the cells cannot recover. Because of this, to be able to analyze the impact of UV irradiation on mitotic progression in these mutants, we decided to reduce the UV dose for these double mutants to half of that for the other strains. As seen in Fig. 4, even at half the dose given to the other strains (120 J/m^2), the *myh1 rad1* double mutants undergo an even more pronounced mitotic burst than *rad1* mutants, starting earlier and reaching higher septation indices.

When examined by DAPI staining, the *myh1 rad1* double mutants exposed to UV exhibited a very high proportion of chromosomal aberrations; the fraction of cells carrying such aberrations exceeded 25%. This figure includes cells with fragmented chromosomal material (12%), bisected nuclei (3%), and missegregated chromosomes (7%) (Fig. 3B and data not shown). It should be noted the other strains examined (wt, *myh1*, and *rad1*) displayed far lower rates of chromosome aberrations (<0.5% total aberrations in wt and *myh1*; 6% in *rad1*) even though they had been exposed to twice the UV dose as *myh1 rad1* (Fig. 3B and data not shown).

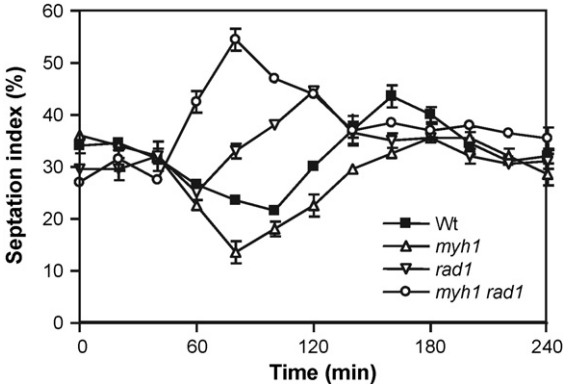

Fig. 4. The cell cycle checkpoint response is severely defective in *rad1 myh1* double mutants. Septation index graphs for wt, *myh1*, *rad1*, and *myh1 rad1* mutants after UV irradiation. Error bars show ±1 standard deviation from two counts. The UV dose was 240 J/m^2 for all strains except the *myh1 rad1* double mutant, which was exposed to 120 J/m^2.

4. Discussion

Previous phenotypic investigations of *E. coli mutY* and *S. pombe myh1* mutants have focused on their sensitivity to oxidative agents, in view of the demonstrated role of MutY homologs in elimination of mispaired bases opposite 8-oxoG, a recognized oxidative DNA damage. We now show that Myh1 is also involved in repair of UV-induced damage. This is demonstrated through the moderately enhanced UV sensitivity of many *myh1* double mutants, and also through the activation of the checkpoint response at lower UV doses (or a more pronounced cell elongation at a fixed dose) in *myh1* single mutants. The latter can be explained by a higher level of residual DNA damage in the *myh1* mutants at a certain UV dose.

We specifically found strong interactions between *rad1* and *rad9* on one hand, and *myh1* on the other, but only a weak enhancement of sensitivity when combining *myh1* with other checkpoint mutations. We find principally two ways of rationalizing this phenomenon. First, it is possible to speculate that Myh1 and these sensor complex proteins function in different pathways, which work towards the same goal of DNA damage elimination with some redundancy. When one gene product is missing from both pathways, neither pathway is operative and the double mutant cell is

highly sensitive to DNA damage. Second, one could think that Myh1 could bind asymmetrically to the 9-1-1 complex. Indeed, it has been shown that Myh1 physically associates with the 9-1-1 complex in fission yeast [7] and in mammalian cells [8]. Other asymmetric associations between the 9-1-1 complex and Myh1 or other proteins are conceivable. It has been reported that the Myh1–Hus1 interaction is selectively enhanced by H_2O_2 treatment [7]. Similarly, human clamp loader hRad17 interacts more strongly with hHus9 than with the two other 9-1-1 complex components [29]. It has been suggested that Myh1 acts as an adapter that is involved both in DNA damage recognition and in recruiting 9-1-1 proteins to the damaged site [7].

The gross morphological defects of the *myh1 rad1* double mutant are not readily explained, as neither *myh1*$^+$ nor *rad1*$^+$ have previously been associated with cell shape abnormalities. This could indicate so far unrecognized roles in cell integrity maintenance for the checkpoint pathway. It should be emphasized that the *myh1 rad1* double mutant is not obviously sensitive to several non-genotoxic agents (Fig. 2A), nor does it have a marked slow growth phenotype (Fig. 2B), indicating that it does not have gross general defects. It is interesting to note, however, that homozygous *myh ogg1* double mutant mouse cells recently have been shown to display multiple centrosomes and multipolar spindles [30]. This indicates a possible explanation for the chromosome segregation defects of the *S. pombe myh1 rad1* double mutants upon DNA damage. Defects in the microtubular network may also impinge on the cell shape abnormalities of this mutant.

The genetic interaction of *myh1* with *rhp51* is indicative of an involvement of Myh1 in recombinative repair, possibly following long-patch BER which requires flap exonuclease (FEN) to create a ligatable single-strand nick following strand displacement DNA synthesis. Both Myh1 and FEN exonuclease physically interact with the 9-1-1 complex; furthermore long-patch BER proteins also interact with the DNA polymerase clamp loader, PCNA [31], and hMYH interacts with proteins involved in long-patch BER including apurinic/apyrimidinic endonuclease 1, PCNA, and replication protein A [32]. It is possible to imagine that Myh1 creates DNA repair intermediates that are normally processed further by Rhp51. For instance, this could consist of unrepaired single-strand breaks in *rhp51* single mutants, arising from Myh1 eliminating adenine opposite 8-oxoG, given that UV produces a limited amount of intracellular oxidative stress. In an *rhp51* single mutant, these potentially cytotoxic intermediates would accumulate, in part explaining the reduced UV resistance and slow growth. In the *myh1 rhp51* double mutant both would be alleviated. In support of the view that such structures can affect long-patch BER, it has been shown that the placement of an 8-oxoG residue juxtaposed to an abasic site will inhibit FEN activity [33].

Our work extends the range of DNA damaging agents where Myh1 has a role in repair. The fact that *myh1 rad1* double mutants are also highly sensitive to HU raises the question if Myh1 can also play a role in activating recovery of DNA replication. It is known that PCNA and the 9-1-1 complex co-localize and physically interact [34–36]. Binding of Myh1 to PCNA [32] could hypothetically occur at the same time as to the 9-1-1 complex through different protein domains. This could be instrumental in linking detection of aberrant DNA structures arising during DNA replication block to activation of checkpoint signaling. From this perspective, it will be interesting to pursue potential genetic interactions between *myh1*$^+$ and *pcn1*$^+$, encoding fission yeast PCNA. The selective genetic interaction of *myh1* with *rad1* and *rad9* also raises the question if application of different external stress conditions and genotoxic agents will reveal interactions between *myh1* and other checkpoint mutations, primarily mutations affecting the third component of the 9-1-1 complex, *hus1*. Further elucidation of the role of eukaryotic MutY homologs in different DNA repair pathways will be important for understanding of its role in mutagenesis and carcinogenesis.

Conflicts of Interest

None.

Acknowledgement

This work was supported by the Swedish Cancer Fund (07-0759).

References

[1] H. Nilsen, H.E. Krokan, Base excision repair in a network of defence and tolerance, Carcinogenesis 22 (2001) 987–998.
[2] M.L. Michaels, C. Cruz, A.P. Grollman, J.H. Miller, Evidence that MutY and MutM combine to prevent mutations by an oxidatively damaged form of guanine in DNA, Proc. Natl. Acad. Sci. U.S.A. 89 (1992) 7022–7025.
[3] Y. Nghiem, M. Cabrera, C.G. Cupples, J.H. Miller, The mutY gene: a mutator locus in *Escherichia coli* that generates G.C–T.A transversions, Proc. Natl. Acad. Sci. U.S.A. 85 (1988) 2709–2713.
[4] A.L. Lu, W.P. Fawcett, Characterization of the recombinant MutY homolog, an adenine DNA glycosylase, from yeast *Schizosaccharomyces pombe*, J. Biol. Chem. 273 (1998) 25098–25105.
[5] T. Doi, S. Yonekura, K. Tano, S. Yasuhira, S. Yonei, Q.M. Zhang, The *Schizosaccharomyces pombe* homolog (SpMYH) of the *Escherichia coli* MutY is required for removal of guanine from 8-oxoguanine/guanine mispairs to prevent G:C to C:G transversions, J. Radiat. Res. (Tokyo) 46 (2005) 205–214.
[6] D.Y. Chang, Y. Gu, A.L. Lu, Fission yeast (*Schizosaccharomyces pombe*) cells defective in the MutY-homologous glycosylase activity have a mutator phenotype and are sensitive to hydrogen peroxide, Mol. Genet. Genomics 266 (2001) 336–342.
[7] D.Y. Chang, A.L. Lu, Interaction of checkpoint proteins Hus1/Rad1/Rad9 with DNA base excision repair enzyme MutY homolog in fission yeast, *Schizosaccharomyces pombe*, J. Biol. Chem. 280 (2005) 408–417.
[8] G. Shi, D.Y. Chang, C.C. Cheng, X. Guan, C. Venclovas, A.L. Lu, Physical and functional interactions between MutY glycosylase homologue (MYH) and checkpoint proteins Rad9–Rad1–Hus1, Biochem. J. 400 (2006) 53–62.
[9] D.Y. Chang, A.L. Lu, Functional interaction of MutY homolog with proliferating cell nuclear antigen in fission yeast, *Schizosaccharomyces pombe*, J. Biol. Chem. 277 (2002) 11853–11858.
[10] M.P. Thelen, C. Venclovas, K. Fidelis, A sliding clamp model for the Rad1 family of cell cycle checkpoint proteins, Cell 96 (1999) 769–770.
[11] Y. Gu, A. Parker, T.M. Wilson, H. Bai, D.Y. Chang, A.L. Lu, Human MutY homolog, a DNA glycosylase involved in base excision repair, physically and functionally interacts with mismatch repair proteins human MutS homolog 2/human MutS homolog 6, J. Biol. Chem. 277 (2002) 11135–11142.
[12] H. Bai, A.L. Lu, Physical and functional interactions between *Escherichia coli* MutY glycosylase and mismatch repair protein MutS, J. Bacteriol. 189 (2007) 902–910.
[13] N. Al-Tassan, N.H. Chmiel, J. Maynard, N. Fleming, A.L. Livingston, G.T. Williams, A.K. Hodges, D.R. Davies, S.S. David, J.R. Sampson, J.P. Cheadle, Inherited variants of MYH associated with somatic G:C → T:A mutations in colorectal tumors, Nat. Genet. 30 (2002) 227–232.
[14] G. Kanter-Smoler, J. Björk, K. Fritzell, Y. Engwall, B. Hallberg, G. Karlsson, H. Grönberg, P. Karlsson, A. Wallgren, J. Wahlstrom, R. Hultcrantz, M. Nordling, Novel findings in Swedish patients with MYH-associated polyposis: mutation detection and clinical characterization, Clin. Gastroenterol. Hepatol. 4 (2006) 499–506.
[15] M.E. Croitoru, S.P. Cleary, N. Di Nicola, M. Manno, T. Selander, M. Aronson, M. Redston, M. Cotterchio, J. Knight, R. Gryfe, S. Gallinger, Association between biallelic and monoallelic germline MYH gene mutations and colorectal cancer risk, J. Natl. Cancer. Inst. 96 (2004) 1631–1634.
[16] A. de la Chapelle, Genetic predisposition to colorectal cancer, Nat. Rev. Cancer 4 (2004) 769–780.
[17] C. Fleischmann, J. Peto, J. Cheadle, B. Shah, J. Sampson, R.S. Houlston, Comprehensive analysis of the contribution of germline MYH variation to early-onset colorectal cancer, Int. J. Cancer 109 (2004) 554–558.
[18] Y. Xie, H. Yang, C. Cunanan, K. Okamoto, D. Shibata, J. Pan, D.E. Barnes, T. Lindahl, M. McIlhatton, R. Fishel, J.H. Miller, Deficiencies in mouse *Myh* and *Ogg1* result in tumor predisposition and G to T mutations in codon 12 of the K-ras oncogene in lung tumors, Cancer Res. 64 (2004) 3096–3102.
[19] K. Sakamoto, Y. Tominaga, K. Yamauchi, Y. Nakatsu, K. Sakumi, K. Yoshiyama, A. Egashira, S. Kura, T. Yao, M. Tsuneyoshi, H. Maki, Y. Nakabeppu, T. Tsuzuki, *MUTYH*-null mice are susceptible to spontaneous and oxidative stress induced intestinal tumorigenesis, Cancer Res. 67 (2007) 6599–6604.
[20] A.L. Goldstein, J.H. McCusker, Three new dominant drug resistance cassettes for gene disruption in *Saccharomyces cerevisiae*, Yeast 15 (1999) 1541–1553.
[21] J. Bähler, J.Q. Wu, M.S. Longtine, N.G. Shah, A. McKenzie III, A.B. Steever, A. Wach, P. Philippsen, J.R. Pringle, Heterologous modules for efficient and versatile PCR-based gene targeting in *Schizosaccharomyces pombe*, Yeast 14 (1998) 943–951.

[22] F. Sherman, Getting started with yeast, Meth. Enzymol. 194 (1991) 3–21.
[23] J. Warringer, E. Ericson, L. Fernandez, O. Nerman, A. Blomberg, High-resolution yeast phenomics resolves different physiological features in the saline response, Proc. Natl. Acad. Sci. U.S.A. 100 (2003) 15724–15729.
[24] S. Moreno, A. Klar, P. Nurse, Molecular genetic analysis of the fission yeast *Schizosaccharomyces pombe*, Meth. Enzymol. 194 (1991) 795–823.
[25] A. Dahlkvist, G. Kanter-Smoler, P. Sunnerhagen, The *RCK1* and *RCK2* protein kinase genes from *Saccharomyces cerevisiae* suppress cell cycle checkpoint mutations in *Schizosaccharomyces pombe*, Mol. Gen. Genet. 246 (1995) 316–326.
[26] G. Jimenez, J. Yucel, R. Rowley, S. Subramani, The *rad3*$^{+}$ gene of *Schizosaccharomyces pombe* is involved in multiple checkpoint functions and in DNA repair, Proc. Natl. Acad. Sci. U.S.A. 89 (1992) 4952–4956.
[27] F. Al-Khodairy, A.M. Carr, DNA repair mutants defining G2 checkpoint pathways in *Schizosaccharomyces pombe*, Embo J. 11 (1992) 1343–1350.
[28] B.A. Moser, J.M. Brondello, B. Baber-Furnari, P. Russell, Mechanism of caffeine-induced checkpoint override in fission yeast, Mol. Cell. Biol. 20 (2000) 4288–4294.
[29] V.P. Bermudez, L.A. Lindsey-Boltz, A.J. Cesare, Y. Maniwa, J.D. Griffith, J. Hurwitz, A. Sancar, Loading of the human 9-1-1 checkpoint complex onto DNA by the checkpoint clamp loader hRad17-replication factor C complex in vitro, Proc. Natl. Acad. Sci. U.S.A. 100 (2003) 1633–1638.
[30] Y. Xie, H. Yang, J.H. Miller, D.M. Shih, G.G. Hicks, J. Xie, R.P. Shiu, Cells deficient in oxidative DNA damage repair genes *Myh* and *Ogg1* are sensitive to oxidants with increased G2/M arrest and multinucleation, Carcinogenesis 29 (2008) 722–728.
[31] E. Friedrich-Heineken, M. Toueille, B. Tannler, C. Burki, E. Ferrari, M.O. Hottiger, U. Hubscher, The two DNA clamps Rad9/Rad1/Hus1 complex and proliferating cell nuclear antigen differentially regulate flap endonuclease 1 activity, J. Mol. Biol. 353 (2005) 980–989.
[32] A. Parker, Y. Gu, W. Mahoney, S.H. Lee, K.K. Singh, A.L. Lu, Human homolog of the MutY repair protein (hMYH) physically interacts with proteins involved in long patch DNA base excision repair, J. Biol. Chem. 276 (2001) 5547–5555.
[33] H. Budworth, I.I. Dianova, V.N. Podust, G.L. Dianov, Repair of clustered DNA lesions. Sequence-specific inhibition of long-patch base excision repair be 8-oxoguanine, J. Biol. Chem. 277 (2002) 21300–21305.
[34] P. Meister, M. Poidevin, S. Francesconi, I. Tratner, P. Zarzov, G. Baldacci, Nuclear factories for signalling and repairing DNA double strand breaks in living fission yeast, Nucleic Acids Res. 31 (2003) 5064–5073.
[35] K. Dahm, U. Hubscher, Colocalization of human Rad17 and PCNA in late S phase of the cell cycle upon replication block, Oncogene 21 (2002) 7710–7719.
[36] V. Ellison, B. Stillman, Biochemical characterization of DNA damage checkpoint complexes: clamp loader and clamp complexes with specificity for 5′ recessed DNA, PLoS. Biol. 1 (2003) E33.